Carbohydrate Research, 66 (1978) 43–52

MOLECULAR STRUCTURES FOR MICROBIAL POLYSACCHARIDES: X-RAY DIFFRACTION RESULTS FROM *Klebsiella* SEROTYPE K57 CAPSULAR POLYSACCHARIDE*

DAVID H. ISAAC, KENN H. GARDNER†, EDWARD D. T. ATKINS,
University of Bristol, H. H. Wills Physics Laboratory, Bristol BS8 1TL (Great Britain)

URSULA ELSASSER-BEILE, AND STEPHAN STIRM,
Max-Planck-Institut für Immunbiologie, 78 Freiburg-Zahringen, Postfach 1169 (G.F.R.)
(Received June 4th, 1976; accepted for publication in revised form, October 3rd, 1977)

ABSTRACT

Fibre X-ray diffraction patterns have been obtained from oriented, semi-crystalline films of the *Klebsiella* capsular polysaccharide serotype K57. K57 is a polytetrasaccharide that contains galactosyluronic acid, mannosyl, and galactosyl residues in the backbone, and an additional mannosyl group as a side-appendage. The simplest interpretation of the diffraction pattern is that the molecule crystallizes as a three-fold helix with an axially projected repeat of 1.143 nm which correlates directly with the chemical repeat. The chain is highly extended, even though it incorporates a 1,2-diaxial linkage in the main backbone. Molecular models have been built using least-squares techniques to minimise interatomic compression and simultaneously meet the observed helical parameters. These models have been compared with the experimental data by using cylindrically averaged, Fourier-transform calculations.

INTRODUCTION

A wide variety of bacteria produce extracellular polysaccharides that surround the cell wall, either attached to the bacteria, or more freely dispersed in the culture fluid. Each cell produces a specific polysaccharide with a regularly repeating sequence of at least two saccharide units. These polysaccharides are highly charged, generally containing uronic acid or pyruvate acetal groups, and this polar nature is thought to provide the polysaccharides with a multi-functional role. In particular, the charged groups bind large quantities of water and ions, giving to the cell surface a slimy or gel-like nature that provides shock absorption and protection against mechanical damage. In addition, the presence of bound water on the cell surface prevents dehydration of the cell and provides an accessible store from which the cell is easily

*Dedicated to Dr. Elizabeth Percival.
†Present address: Department of Macromolecular Science, Case Western Reserve University, Cleveland, Ohio 44106, U.S.A.

able to absorb water and ions. The polysaccharides also protect the cell against attack by bacteriophages, in general, but are degraded by specific phages that are then able to invade the host bacterial cell. Indeed, it is this specific antigenic property which is used to classify this group of polysaccharides.

It is only recently that the chemical compositions, and in some cases the details of linkage and sequence, have been determined for some of these polysaccharides. In particular, the carbohydrate components from the bacteria of the genus *Klebsiella* have been intensively investigated, and the complete repeating-sequences of a number of these have now been established. Extracellular polysaccharides from various other bacteria, *e.g.*, *Escherichia coli*, *Leuconostoc mesenteroides*, and *Xanthomonas campestris*, have also been characterised, but we chose to investigate those from the genus *Klebsiella*, since this family contains a large variety of chemical structures, of which a substantial number have already been completely elucidated.

The primary structure of *Klebsiella* K57 capsular polysaccharide consists[1] of tetrasaccharide repeating-units **1**.

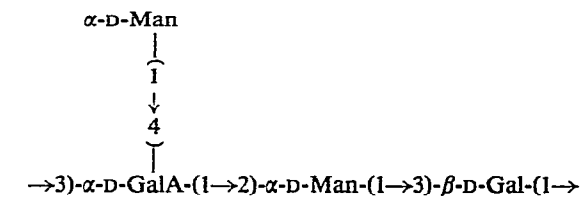

1

It is anticipated that all of the sugar residues are in the normal $^4C_1$ conformation. This results in a backbone linkage-geometry of Gal-(1eq→3eq)-GalA-(1ax→2ax)-Man-(1ax→3eq)-Gal, with the side-chain attached Man-(1ax→4ax)-GalA as shown in Fig. 1.

Recently, we have obtained X-ray fibre diffraction patterns from samples of this polysaccharide, and by using the helical parameters from such patterns we have investigated the molecular conformation of the K57 molecule with computerised model-building procedures.

MATERIALS AND METHODS

Materials. — *Klebsiella* 4425/51 (05:K57) was grown on $D_{1.5}$ agar[2], and the capsular polysaccharide (sodium salt) was isolated by the phenol–water–cetyltrimethylammonium bromide procedure[3,4]. It contained <0.8% of nucleic acid and <0.1% of protein. A sufficiently pure preparation of K57 glycan was also obtained by phenol–water extraction and direct lyophilization of the water phase following prolonged sedimentation (2 × 12 h at 105,000 *g*) of the cell-wall lipopolysaccharide.

Fibre preparations[5]. — A viscous solution (~1% w/w) of the sodium salt form was allowed to dry on a smooth glass slide coated with "Repelcote" (dichlorodimethylsiloxane in carbon tetrachloride) to prevent the sample sticking to the slide.

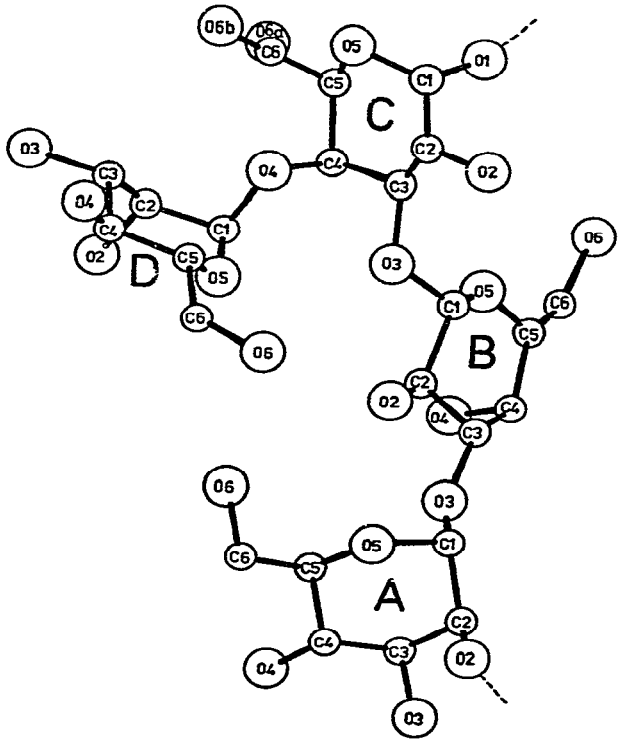

Fig. 1. The tetrasaccharide, chemical repeating-unit of *Klebsiella* K57 polysaccharide, showing the atom labelling: A, α-D-mannose; B, β-D-galactose; C, α-D-galacturonic acid; and D, α-D-mannose.

The film was removed from the slide and cut into strips (~2 mm wide), which were then stretched under constant load and at high, relative humidities (in the range 90 to 98%). The humidity was controlled by placing saturated salt solutions in the desiccator. To achieve well-oriented samples, it was found that stretching by a factor of 2–3 was necessary.

X-Ray diffraction. — X-Ray fibre diffraction patterns were recorded on flat film (Ilford Industrial G) by using pinhole-collimated (250-μm diameter), nickel-filtered CuK_α radiation from an Elliott rotating-anode X-ray generator. High, relative humidity was maintained during exposure by bubbling hydrogen through a salt solution before passage through the camera which also contained a saturated salt solution. Photographs of specimens in a number of orientations about the stretch axis were all similar, indicating cylindrical symmetry. The diffraction patterns were calibrated by dusting the sample with finely powdered crystals of calcite (characteristic spacing, 0.3035 nm).

Molecular model building. — The atom labelling for the tetrasaccharide repeating-unit is shown in Fig. 1. Molecular models were generated by using a linked-atom description similar to that first reported by Arnott and Wonacott[6]. The

positions of the atoms were defined in terms of the bond lengths, bond angles, and torsion angles of the molecule. Stereochemical parameters for pyranoid rings in the standard $^4C_1$ chair are based on average co-ordinates for α-D-glucosyl and β-D-glucosyl residues given by Arnott and Scott[7]. Bond lengths and bond angles were held constant, including the angles for the glycosidic bridges which were assigned a value of 116.5°. This defines the pyranoid rings and the side-groups as rigid bodies, and leaves the glycosidic torsion angles, and also the torsion angles that define the orientation of the hydroxymethyl and carboxyl groups, as explicit variables. These parameters were varied to produce a model with the appropriate helical symmetry and pitch, and with the minimum amount of non-bonded steric compression. This was accomplished, using the technique reported by Guss *et al.*[8], by minimizing Φ,

where $\Phi = \sum \varepsilon_j + \sum \lambda_h G_h$. (*1*)

The first summation in Φ ensures good stereochemistry in the model by optimizing non-bonded interactions between atom pairs. Both repulsive and attractive interactions may be incorporated into this description. The second summation contains exact constraints which ensure helix pitch and symmetry, molecular continuity, and any other constraints to be imposed on the model. The details of this formalization have been given by Guss *et al.*[8] and by Sheehan *et al.*[9].

Calculated intensity distribution. — In an attempt to distinguish between models using our experimental diffraction data, cylindrically averaged Fourier-transforms of various structures were calculated by using the equations of Franklin and Klug[10]. Atomic scattering factors were calculated by using an analytical expression given in International Tables[11]. These values were then modified to approximate the effect of disordered water in the voids between chains, using the expression given by Arnott and Hukins[12]. Calculations of intensities were made at intervals of 0.3 nm^{-1} out to 2.7 nm^{-1}, and on layer lines 0 to 6. It was found, in practice, that the contributions from Bessel functions of order greater than 12 were negligible.

RESULTS AND DISCUSSION

Fig. 2 shows the X-ray fibre diffraction pattern obtained from the sodium salt of *Klebsiella* K57 polysaccharide. This photograph has a layer-line spacing of 3.429 nm, with meridional reflections occurring only on those layer lines with $l = 3n$. This is most simply interpreted as being due to a three-fold helical structure with a projected chemical repeating-unit of 1.143 nm. This projected repeat may be compared with the absolute-maximum theoretical extension of 1.26 nm, which would occur if all the vectors joining successive glycosidic oxygen atoms of the backbone were to line up precisely. The experimental repeat is ~10% less than this maximum extension, a feature in common with a large number of polysaccharides (see, *e.g.*, Atkins *et al.*[13]), and indicates a fairly extended structure.

The arrangement of helices in a plane perpendicular to the helix axis is not so clearly defined. Several row lines are observed, but no unequivocal indexing of the

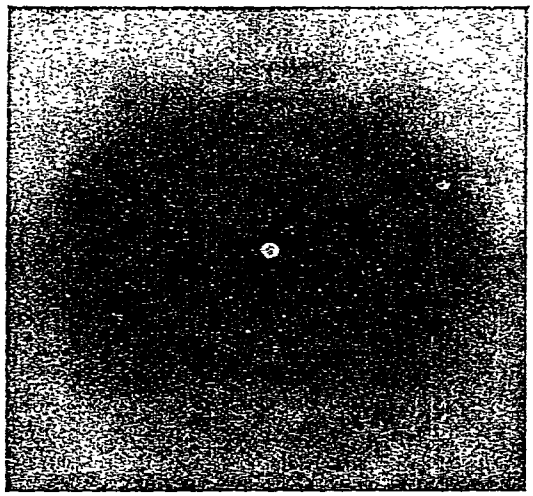

Fig. 2. X-Ray fibre diffraction pattern of the sodium salt form of *Klebsiella* K57 polysaccharide.

unit cell is possible. Our best guess, bearing in mind the three-fold nature of the helices, is that molecules pack together in a slightly distorted hexagonal or trigonal lattice.

Interchain packing is not well-defined and this situation suggests that interactions between molecules are not significant in determining the conformations of individual chains. Therefore, our model-building investigations have been limited to the consideration of isolated helices. Initially, both left- and right-handed three-fold helices were built to fit the observed helical pitch. Various starting positions were considered for each of the glycosidic linkages, since, as in any least-squares routine, the final structure is intimately related to the initial model. The two major considerations for the starting conformational angles were the absence of steric compression and the potential formation of stabilizing inter-residue hydrogen-bonds. Thus, as starting models for the least-squares "minimisation of energy" refinement, we considered firstly helices which incorporated a variety of hydrogen bonds, and secondly conformations in which the glycosidic torsion angles were set to values near the centre of their sterically allowed regions. From the various structures that were generated when these trial models were refined by the "soft" atom approach, the best right-handed and best left-handed conformations are illustrated (Fig. 3, and Tables I and II).

For the right-handed model (Fig. 3*a*), no hydrogen bonds are incorporated into the backbone and no short contacts occur. Although some of the other right-handed starting conformations refined to structures that included hydrogen bonds, unacceptable interatomic contacts were present in all cases.

In the best left-handed helix (Fig. 3*b*), two hydrogen bonds are incorporated, namely [α-D-Man-O(5)–H-O(2)-β-D-Gal] and [α-D-GalA-O(2)–H-O(3)-α-D-Man], but two short contacts appear (O → H of 0.212 nm, and O → C of 0.265 nm). The other

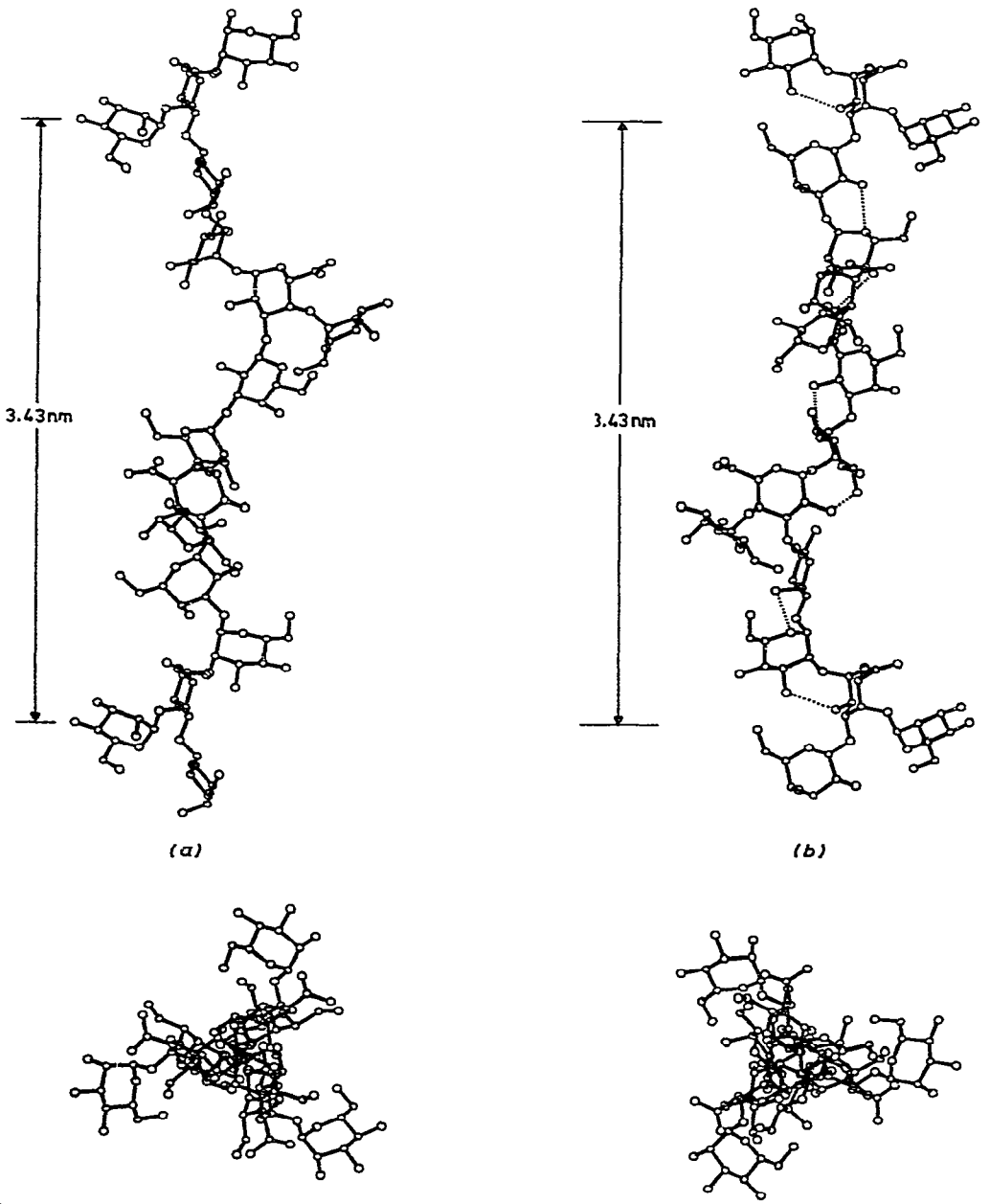

Fig. 3. Projections of molecular models of *Klebsiella* K57 polysaccharide with three-fold helical structures repeating in 3.43 nm: (*a*) the best right-handed model; and (*b*) the best left-handed model; the dotted lines show the hydrogen bonds that may be incorporated in this model (see text).

starting conformations refined to models very similar to this structure. A further hydrogen bond (from O-6 of the α-D-Man side-group to O-2 of β-D-Gal) could be incorporated into this model without significant change in the backbone.

Although the X-ray diffraction pattern gives some discrete Bragg reflections, we have not been able to assign a unit cell and hence index each reflection. Thus, the

TABLE I

CARTESIAN CO-ORDINATES OF THE RIGHT-HANDED MODEL (FIG. 3*a*)

Atom	*x* (*nm*)	*y* (*nm*)	*z* (*nm*)	*Atom*	*x* (*nm*)	*y* (*nm*)	*z* (*nm*)
α-D-*Mannose* (*residue A*)				β-D-*Galactose* (*residue B*)			
C-1	0.0418	−0.0001	1.2385	C-1	−0.1995	−0.0073	0.8123
C-2	−0.0262	0.0108	1.3744	C-2	−0.1261	0.0734	0.9186
C-3	−0.0309	0.1558	1.4201	C-3	−0.0946	−0.0136	1.0393
C-4	0.1085	0.2171	1.4166	C-4	−0.2212	−0.0816	1.0900
C-5	0.1719	0.1959	1.2798	C-5	−0.2915	−0.1538	0.9756
C-6	0.3162	0.2416	1.2745	C-6	−0.4241	−0.2139	1.0171
O-1	−0.0383	0.0669	1.1430	O-1	−0.2377	0.0790	0.7104
O-2	0.0455	−0.0667	1.4698	O-2	−0.0069	0.1274	0.8627
O-3	−0.0832	0.1626	1.5528	O-3	−0.0383	0.0669	1.1430
O-4	0.1018	0.3572	1.4424	O-4	−0.3088	0.0163	1.1454
O-5	0.1713	0.0572	1.2468	O-5	−0.3189	−0.0621	0.8685
O-6	0.3749	0.2171	1.1468	O-6	−0.4772	−0.3000	0.9165
H-1	0.0497	−0.1050	1.2096	H-1	−0.1348	−0.0889	0.7769
H-2	−0.1277	−0.0313	1.3682	H-2	−0.1886	0.1583	0.9499
H-3	−0.0978	0.2130	1.3540	H-3	−0.0207	−0.0901	1.0111
H-4	0.1712	0.1701	1.4938	H-4	−0.1949	−0.1546	1.1679
H-5	0.1152	0.2518	1.2039	H-5	−0.2274	−0.2353	0.9387
H-6a	0.3747	0.1875	1.3503	H-6a	−0.4967	−0.1333	1.0354
H-6b	0.3212	0.3497	1.2947	H-6b	−0.4106	−0.2726	1.1092
α-D-*Galacturonic acid* (*residue C*)				α-D-*Mannose* (*residue D*)			
C-1	−0.1779	0.0955	0.3402	C-1	−0.5541	0.0453	0.6512
C-2	−0.1793	0.1422	0.4851	C-2	−0.6942	0.0554	0.5921
C-3	−0.2247	0.0297	0.5769	C-3	−0.7223	0.1976	0.5461
C-4	−0.3581	−0.0268	0.5298	C-4	−0.6967	0.2962	0.6592
C-5	−0.3501	−0.0646	0.3825	C-5	−0.5574	0.2749	0.7171
C-6	−0.4838	−0.1077	0.3259	C-6	−0.5314	0.3600	0.8396
O-1	−0.0799	−0.0058	0.3269	O-1	−0.4603	0.0709	0.5483
O-2	−0.0494	0.1875	0.5212	O-2	−0.7899	0.0174	0.6903
O-3	−0.2377	0.0790	0.7104	O-3	−0.8582	0.2080	0.5029
O-4	−0.4603	0.0709	0.5483	O-4	−0.7061	0.4303	0.6115
O-5	−0.3069	0.0475	0.3057	O-5	−0.5416	0.1390	0.7570
O-6a	−0.5628	−0.0322	0.2717	O-6	−0.4011	0.3372	0.8932
O-6b	−0.5087	−0.2363	0.3402	H-1	−0.5373	−0.0556	0.6891
H-1	−0.1509	0.1785	0.2749	H-2	−0.7039	−0.0152	0.5084
H-2	−0.2477	0.2278	0.4954	H-3	−0.6574	0.2221	0.4607
H-3	−0.1491	−0.0502	0.5772	H-4	−0.7719	0.2818	0.7383
H-4	−0.3828	−0.1164	0.5886	H-5	−0.4819	0.2998	0.6410
H-5	−0.2789	−0.1475	0.3696	H-6a	−0.6054	0.3360	0.9173
				H-6b	−0.5396	0.4664	0.8128

best comparison between the experimental data and model building can only be done on the basis of cylindrically averaged, Fourier transforms. Although such calculations are not expected to be representative of the diffraction pattern, since this shows sampling of reciprocal space, it might be possible from the molecular transform to

TABLE II

CARTESIAN CO-ORDINATES OF THE LEFT-HANDED MODEL (FIG. 3*b*)

Atom	*x* (*nm*)	*y* (*nm*)	*z* (*nm*)	*Atom*	*x* (*nm*)	*y* (*nm*)	*z* (*nm*)
α-D-*Mannose* (*residue A*)				*β*-D-*Galactose* (*residue B*)			
C-1	0.0830	0.0196	1.2209	C-1	0.0882	0.0743	0.7731
C-2	0.0435	0.0550	1.3637	C-2	0.1369	0.0747	0.9174
C-3	0.1467	0.1478	1.4260	C-3	0.0275	0.1250	1.0105
C-4	0.2861	0.0876	1.4145	C-4	−0.0247	0.2598	0.9627
C-5	0.3150	0.0488	1.2701	C-5	−0.0645	0.2517	0.8157
C-6	0.4462	−0.0251	1.2546	C-6	−0.1065	0.3857	0.7591
O-1	0.0795	0.1376	1.1430	O-1	0.1950	0.0406	0.6909
O-2	0.0337	−0.0640	1.4412	O-2	0.1777	−0.0567	0.9537
O-3	0.1148	0.1695	1.5636	O-3	0.0795	0.1376	1.1430
O-4	0.3846	0.1817	1.4569	O-4	0.0767	0.3587	0.9791
O-5	0.2127	−0.0380	1.2217	O-5	0.0465	0.2061	0.7368
O-6	0.4692	−0.0645	1.1194	O-6	−0.1669	0.3723	0.6305
H-1	0.0115	−0.0515	1.1795	H-1	0.0034	0.0049	0.7632
H-2	−0.0560	0.1019	1.3637	H-2	0.2252	0.1397	0.9262
H-3	0.1444	0.2450	1.3746	H-3	−0.0550	0.0523	1.0127
H-4	0.2930	−0.0016	1.4786	H-4	−0.1127	0.2883	1.0222
H-5	0.3187	0.1393	1.2078	H-5	−0.1488	0.1820	0.8042
H-6a	0.4451	−0.1156	1.3171	H-6a	−0.0184	0.4507	0.7492
H-6b	0.5290	0.0401	1.2861	H-6b	−0.1794	0.4328	0.8267
α-D-*Galacturonic acid* (*residue C*)				α-D-*Mannose* (*residue D*)			
C-1	0.1445	−0.0285	0.3254	C-1	0.5000	0.0871	0.6407
C-2	0.1470	−0.0559	0.4752	C-2	0.6407	0.1145	0.5892
C-3	0.1806	0.0710	0.5520	C-3	0.7039	−0.0134	0.5365
C-4	0.3095	0.1325	0.4993	C-4	0.6980	−0.1231	0.6420
C-5	0.3014	0.1503	0.3482	C-5	0.5554	−0.1394	0.6930
C-6	0.4320	0.1974	0.2879	C-6	0.5454	−0.2367	0.8085
O-1	0.0385	0.0612	0.2982	O-1	0.4194	0.0475	0.5314
O-2	0.0207	−0.1075	0.5157	O-2	0.7205	0.1669	0.6948
O-3	0.1950	0.0406	0.6909	O-3	0.8400	0.0116	0.5007
O-4	0.4194	0.0475	0.5314	O-4	0.7411	−0.2474	0.5870
O-5	0.2696	0.0259	0.2863	O-5	0.5059	−0.0142	0.7400
O-6a	0.5218	0.1229	0.2522	O-6	0.4114	−0.2487	0.8563
O-6b	0.4412	0.3284	0.2765	H-1	0.4581	0.1782	0.6835
H-1	0.1262	−0.1213	0.2713	H-2	0.6368	0.1912	0.5105
H-2	0.2222	−0.1331	0.4972	H-3	0.6504	−0.0464	0.4463
H-3	0.0983	0.1433	0.5413	H-4	0.7642	−0.0970	0.7259
H-4	0.3252	0.2308	0.5462	H-5	0.4912	−0.1759	0.6114
H-5	0.2235	0.2242	0.3241	H-6a	0.6086	−0.2018	0.8915
				H-6b	0.5794	−0.3361	0.7759

eliminate a model if, for example, the calculated transform falls to a very low value at some point where a strong observed reflection occurs. We feel more justified in this approach than in trying to pack the helices into a trial unit-cell based on a hexagonal arrangement.

The cylindrically averaged, Fourier transforms of our two models are shown in Fig. 4. We hesitate to distinguish between them on this evidence, since both transforms are consistent with the data and neither is calculated low in positions where reflections occur.

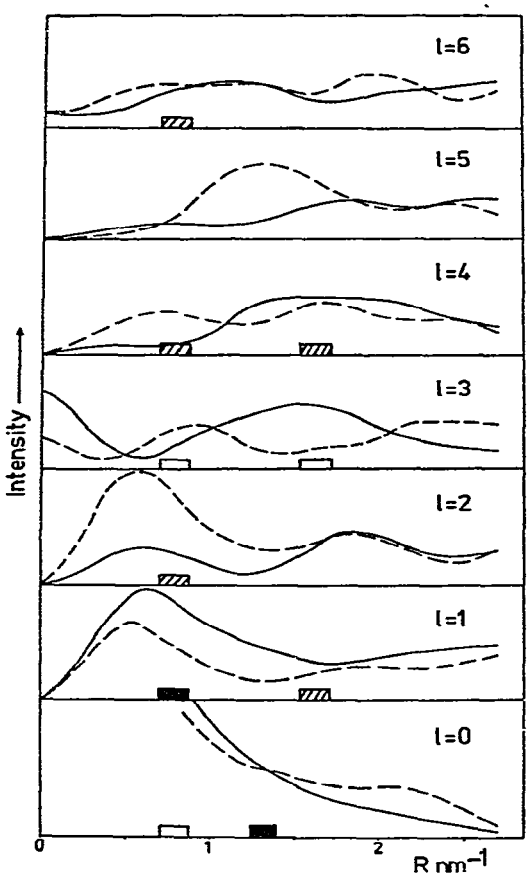

Fig. 4. The cylindrically averaged, Fourier transforms of the two models illustrated in Fig. 3. The broken line shows the transform of the right-handed model, and the solid line that of the left-handed structure. The rectangular boxes represent the positions of the experimentally observed, diffracted intensities. Open boxes represent weak intensity, cross-hatching represents medium intensity, and solid boxes represent strong observed intensities.

CONCLUSIONS

We have presented X-ray diffraction evidence for a regularly repeating, helical structure in *Klebsiella* K57 capsular polysaccharide. The X-ray diffraction pattern is of insufficient quality to determine the lateral arrangement of the molecules, and the details of their interactions in the solid state. However, trial structures have been constructed for isolated helices, and Fourier-transform calculations show that these do not conflict with the observed data. Of the two models illustrated, namely, one right- and one left-handed model, we tend to favour the latter, since this contains stabilizing interchain-bonds. In some highly crystalline samples (*e.g.*, the double helix of hyaluronic acid[9]), such hydrogen bonds are not present; instead, the structure is stabilized by interchain hydrogen bonds. However, for K57, the diffraction pattern suggests that packing together of helices is not well-ordered and hence interchain forces appear to be less important. Such an argument supports our search for stabilized, isolated helical structures, which are expected to pack together in an irregular array. Indeed, it is interesting to speculate that helices built to such criteria (*i.e.*, without interchain considerations) are likely to be more closely related to the conformations occurring in solution and also under *in vivo* conditions.

REFERENCES

1 J. P. KAMERLING, B. LINDBERG, J. LÖNNGREN, AND W. NIMMICH, *Acta Chem. Scand., Ser. B*, 29 (1975) 593–598.
2 S. SCHLECHT AND O. WESTPHAL, *Zentralbl. Bakteriol. Parasitenk. Infektionskr. Hyg., Abt. 1: Orig., Reihe A*, 200 (1966) 241–259.
3 K. JANN, B. JANN, F. ØRSKOV, I. ØRSKOV, AND O. WESTPHAL, *Biochem. Z.*, 342 (1965) 1–22.
4 H. THUROW, Y.-M. CHOY, N. FRANK, H. NIEMANN, AND S. STIRM, *Carbohydr. Res.*, 41 (1975) 241–255.
5 E. D. T. ATKINS, C. F. PHELPS, AND J. K. P. SHEEHAN, *Biochem. J.*, 128 (1972) 1255–1263.
6 S. ARNOTT AND A. WONACOTT, *Polymer*, 7 (1966) 157–166.
7 S. ARNOTT AND W. E. SCOTT, *J. Chem. Soc., Perkin Trans. 2*, (1972) 324–335.
8 J. M. GUSS, D. W. L. HUKINS, P. J. C. SMITH, W. T. WINTER, S. ARNOTT, R. MOORHOUSE, AND D. A. REES, *J. Mol. Biol.*, 95 (1975) 359–384.
9 J. K. P. SHEEHAN, K. H. GARDNER, AND E. D. T. ATKINS, *J. Mol. Biol.*, 117 (1977) 113–135.
10 R. E. FRANKLIN AND A. KLUG, *Acta Crystallogr.*, 8 (1955) 777–780.
11 International Tables for X-Ray Crystallography, Kynoch Press, Birmingham, 1974.
12 S. ARNOTT AND D. W. L. HUKINS, *J. Mol. Biol.*, 81 (1973) 93–105.
13 E. D. T. ATKINS, D. H. ISAAC, I. A. NIEDUSZYNSKI, C. F. PHELPS, AND J. K. P. SHEEHAN, *Polymer*, 15 (1974) 263–271.